ACS OMEGA

Open Access

http://pubs.acs.org/journal/acsodf

Article

Accelerated Testing of PEI-Silica Sorbent Pellets for Direct Air Capture

Harshul V. Thakkar,* Andrew J. Ruba, John A. Matteson, Michael P. Dugas, and Rajinder P. Singh*

Cite This: *ACS Omega* 2024, 9, 45970−45982

Read Online

ACCESS | Metrics & More | Article Recommendations | Supporting Information

ABSTRACT: Amine-based sorbents have shown exceptional CO_2 uptake for direct air capture (DAC). However, amine degradation is a major issue for this class of materials, hindering their deployment for large-scale DAC. In this study, a comprehensive evaluation of polyethylenimine (PEI) sorbents was conducted to understand their degradation under process-relevant environments for the DAC of CO_2. A solvent-minimized silica-supported PEI-sorbent powder synthesis method using centrifugal mixing was developed. Unlike traditional solvent-assisted impregnated sorbent synthesis methods, the centrifugal mixing method enabled a 94% reduction in volatile and toxic organic solvent use in pelletized sorbent synthesis. The pelletized sorbents exhibited CO_2 adsorption capacities consistent with traditional fabrication methods for PEI-based solid sorbents (about 1 mmol/g). The pelletized sorbent degradation behavior was evaluated at three different regeneration temperatures (80, 100, and 120 °C) under nitrogen (N_2), ambient air (21% O_2), and saturated dry and wet (75% relative humidity (RH)) CO_2 environments using fixed-bed breakthrough (BT) experiments. Additionally, accelerated testing (AT) protocols that mimic industrial DAC conditions were developed to assess the long-term stability of the PEI-silica pellets. Our results indicate that the sorbent degrades rapidly (ca. 94% within 24 h) at 120 °C in ambient air (21% O_2), demonstrating the detrimental impact of oxygen when compared to an O_2-free environment. AT performed for 100 h (equivalent to 33, 100, and 100 cycles) continuously at 80, 100, and 120 °C reveals that dry CO_2-induced degradation of the PEI-silica sorbent pellets is 30−40% and 40−50% more than the degradation measured in wet CO_2 and inert (pure N_2) environments.

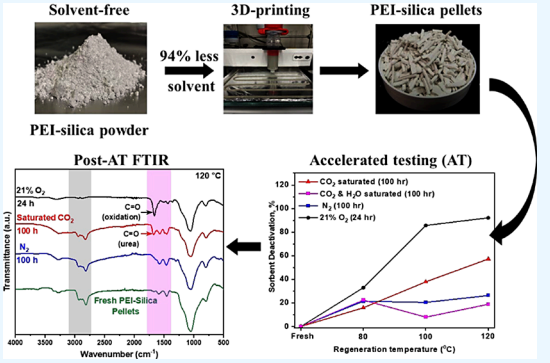

1. INTRODUCTION

Greenhouse gas emission-led climate change is undeniably the biggest threat to our planet. Carbon dioxide (CO_2) removal via direct air capture (DAC) can provide an impactful, engineered approach to combat climate change.[1,2] According to the International Energy Agency (IEA), DAC is expected to remove ca. 85 and 980 million tons (MT) of CO_2 by 2030 and 2050, respectively, to achieve net zero carbon emissions and ensure a global temperature increase of less than 2 °C.[3] Energy-efficient DAC with a longer sorbent lifetime is needed to achieve the U.S. Department of Energy's (DOE) target (< \$100/ton CO_{2eq}) while permanently storing the captured CO_2 in geological formations or providing a carbon source for liquid fuels, polymers, and chemicals in a future fossil fuel-free world.[1,4−8]

Amine-based solid sorbents are leading sorbent materials for DAC of CO_2 as these sorbents have relatively high CO_2 uptake in humid environments compared to liquid sorbents and other solid sorbents such as zeolites, metal−organic frameworks (MOFs), and activated carbon.[2,5,9−13] However, amines are susceptible to oxidative and thermal degradation, greatly hampering their industrial utility. Thermal, oxidative, and CO_2-induced degradation of the sorbent, due to the evaporation of amines, free radical formation by the reaction of O_2 with amines, and the formation of open chain urea, respectively, occurs at regeneration temperatures (≥70 °C).[14] Several efforts have been made to improve the adsorption performance and thermo-oxidative stability of amine-based solid sorbents for DAC, as summarized in Table 1.

Sayari and co-workers studied the impact of regeneration temperature on different molecular weights (M_w) of branched polyethylenimine (PEI) loaded onto SBA-15 using thermogravimetric analysis (TGA) for more than 65 adsorption−desorption cycles.[15] They found that the sorbent with PEI (avg. M_w 400) thermally degraded by 2.6 and 23% at 75 and 120 °C, respectively, under dry nitrogen (N_2). Similarly, weight losses of ca. 23, 4.0, and 1.3% were measured at 120 °C for having PEI molecular weights of 423, 600, and 2500, respectively. Additional results indicated that PEI (M_w 600) sorbents degraded by ca. 25 and 68% under 5% CO_2 balance

Received: June 17, 2024
Revised: September 27, 2024
Accepted: October 23, 2024
Published: November 6, 2024

Table 1. Summary of Amine-Based Sorbents and Their Evaluation Conditions and Degradation Behavior for DAC of CO_2

support material	adsorbent	adsorption gas	CO_2 uptake, $mmol_{CO_2}/g$ sorbent	regeneration gas	regeneration temperature (°C)	number of cycles	total time (h)	%degradation vs. fresh material	ref
SBA-15	BPEI[a], M_w = 423	5% CO_2, bal. N_2	2.9	N_2	75		30	2.6%	15
	BPEI[a], M_w = 600							0.3%	
	LPEI[b], M_w = 2500							0.0%	
	BPEI[a], M_w = 600			5% CO_2 bal. in N_2	85		10	2%	
					105		10	25%	
					120		10	68%	
SBA-15 (fresh)	blended 6700 − 700 M_n LPPI[c], aged	400 ppm of CO_2, bal. He	0.96	He	90	20	33	negligible	16
		10% CO_2, bal. He	1.9					∼4.5%	
SBA-15 (fresh)	6,700 M_n LPPI[c], aged	400 ppm of CO_2, bal. He	2.3	aged in ambient air			∼17,500	∼48%	
SBA-15 (aged)	6,700 M_n LPPI[c], aged						∼17,500	∼10%	
SBA-15	BPEI[a], M_n = 600	400 ppm of CO_2, bal. He	1.3	0.04% CO_2−air (43% RH)	70	30	125	52%	17
				0.04% CO_2−air (dry)		30	125	29%	
				21% O_2, bal. N_2			168	4%	
				21% O_2, bal. N_2 (43% RH)				17%	
				N_2				3%	
				0.04% CO_2 bal. air				80%	
				0.04% CO_2 bal. air (43% RH)				87%	
				0.04% CO_2, bal N_2				2%	
				21% O_2, bal N_2			336	32%	
				N_2				4%	
mesoporous alumina	BPEI[a], M_n = 600	400 ppm of CO_2, bal. He	1.1	21% O_2, bal. N_2 (dry)	120		9	75%	18
				21% O_2, bal. N_2 (18 °C dew point)			8	97%	
				21% O_2, bal. N_2 (30 °C dew point)			8	96%	
macroporous silica	PEI	15% CO_2, 10% H_2O, bal. N_2	2.0	aged under 3% O_2, 15% CO_2, 10% H_2O, bal N_2	110		720	97%	24
	PEI w/2% chelator		2.0					84%	
	EB[d] − PEI		1.6					85%	
	EB[d] − PEI w/2% chelator		1.6					8.2%	
porous silica	0.42EB[d] − TEPA[e]	15%/85% CO_2/N_2	2.5	N_2	90	10		∼7.0%	25
	0.64EB[d] − TEPA[e]		2.0					∼6.4%	
	0.82EB[d] − TEPA[e]		1.6					∼2.6%	
proprietary aminoresin		400 ppm of CO_2, bal. N_2	0.57	N_2, TCSA[f] mode	100	19	95	7.6%	28
			0.52	N_2, TVCSA[g] mode	100	22	99	13%	
			0.53	N_2, TVCSA[g] mode	60	23	103.5	5.7%	
SBA-15	PEI	400 ppm of CO_2, bal. N_2	0.72	N_2	70	10	15	∼3.9%	20
			1.0		80			∼2.5%	
			1.0		90			∼1.3%	
			0.94		110			∼0.8%	
			0.72	24 h thermal treatment + N_2	70		44	∼5.6%	
			1.0		80			∼5.0%	
			1.0		90			∼9.1%	
			0.94		110			∼7.6%	
	TEPA[e]	400 ppm of CO_2, bal N_2	1.3	N_2	70		15	∼0.6%	
			1.7		80			∼0.3%	
			1.8		90			∼0.0%	
			1.7		110			∼1.9%	
			1.3	24 h thermal treatment + N_2	70		44	∼2.2%	
			1.7		80			∼5.3%	
			1.8		90			∼11%	
			1.7		110			∼67%	

[a]Branched polyethylenimine (PEI). [b]Linear polyethylenimine (PEI). [c]Linear poly(propylenimine). [d]Epoxybutane (EB). [e]Tetraethylenepentamine (TEPA). [f]Temperature−concentration swing adsorption. [g]Temperature−vacuum−concentration swing adsorption.

https://doi.org/10.1021/acsomega.4c05639
ACS Omega 2024, 9, 45970−45982

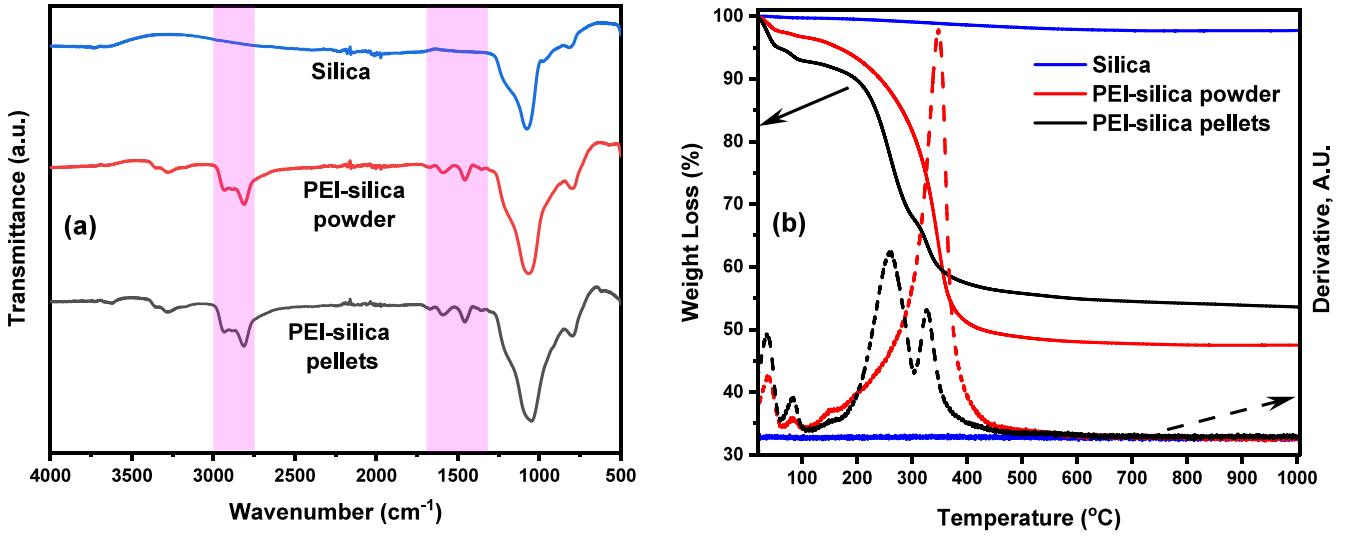

Figure 1. FTIR spectra (a) and thermogravimetric analysis (b) of silica, PEI-silica powder, and PEI-silica pellets.

N_2 mixture at 105 and 120 °C, respectively, when compared to pristine sorbents. This degradation was primarily attributed to the loss of amine groups via urea formation. Rosu et al. used aged (~2 years) linear PEI loaded onto SBA-15 supports and examined its CO_2 performance for DAC on TGA.[16] The results showed that the aged linear PEI showed ~20% lower uptake than fresh linear PEI with stable performance over 20 cycles. Jones and group investigated branched PEI (800 M_w) on γ-Al_2O_3 supports via TGA for 30 cycles at 70 °C.[17] Their findings showed a gradual loss in stability (dry: 29%, humid: 52%) under 0.04% CO_2−air for 45 wt % PEI- γ-Al_2O_3. Most recently, Carneiro et al. assessed the oxidative degradation mechanism of branched PEI under humid DAC conditions.[18] Their results indicated that a radical-initiated autoxidation mechanism governs the PEI-based sorbent degradation due to a primary step of abstraction of hydrogen from C−H bonds, resulting in the release of volatile organic compounds (VOCs) such as ammonia and 2-aminoacetaldehyde at terminal 1° and 2° amines.

To reduce the oxidative and thermal degradation of amine-based solid sorbents for DAC, several approaches have been explored. For example, low-temperature DAC, which adsorbs at subambient temperatures and desorbs at room or low temperatures (60 °C), was proposed.[1,19−22] Rim et al. studied PEI and tetraethylenepentamine (TEPA) loaded onto MIL-101 (Cr) supports for DAC where adsorption and desorption were carried out at −30 °C and 40−60 °C, respectively, using TGA-DSC, volumetric surface area analysis, and porosimetry.[21] They concluded that 30 wt % TEPA-loaded sorbents showed a large working capacity (0.73 mmol/g) for 15 cycles with a low sorbent regeneration temperature (25 °C) due to weak chemisorption-dominant behavior. In another approach to reduce oxidative degradation, small molecules/additives (e.g., epoxides) forming hydroxyl bonds with amines were explored to retard amine oxidation.[23−26] Choi and co-workers modified branched PEI with 1,2-epoxybutane (EB) before loading onto silica supports and assessed its stability in flue gas (15% CO_2, 3% H_2O, 2% Ar, balance N_2) by performing temperature swing adsorption using TGA-MS for 50 cycles. They utilized 0.37 and 0.54 EB-PEI, which is defined by the molar ratio of EB to nitrogen content in PEI. Their results demonstrated that 0.37 and 0.54 EB-PEI-silica retained almost 100% of their working capacity for 50 cycles, even though the actual adsorption capacity reduced from 3.8 mmol/g to ~2 and 1.5 mmol/g, respectively, due to the addition of EB to PEI.[24] Another study used the same additive for TEPA and showed stable performance over 10 cycles using TGA under 15% CO_2 in N_2.[25] Even though amines with additives showed improved oxidative stability, the sorbent showed reduced CO_2 uptake compared to amines without additives, as additives generally do not participate in the capture process.[26]

Several process engineering approaches are proposed to counter the thermal degradation of sorbents, including the use of inert gas purging to minimize the presence of O_2 during desorption. Elfving et.al. evaluated desorption using an inert gas (e.g., nitrogen) at a low temperature (60 °C) on a proprietary sorbent.[27,28] This is the only study, to the authors' knowledge, that carried out cyclic adsorption−desorption on a fixed-bed column for over 20 cycles at 60 and 100 °C regeneration with purge and vacuum. The authors demonstrated that 60 °C is sufficient to reach 85% regeneration with both temperature-swing adsorption (TSA) and temperature−concentration swing adsorption (TCSA). Coupling purge gas use and vacuum in TVSA/TVCSA (V-vacuum) leads to over ca. 90% regeneration. Although a lower specific energy requirement of 4.2 MJ/kg CO_2 was achieved with purge gas and no vacuum, compared to ca. 7.5 MJ/kg CO_2 with mild vacuum for low-concentration CO_2 streams (1−10%), the sorbent degraded by 6% over 23 cycles at 60 °C in TVCSA mode.

There are three basic methods for incorporating amines onto a porous support: impregnation, grafting, and in situ amine loading. Among these, wet impregnation with a solvent is the easiest way to load amines onto a porous support, followed by the evaporation of the solvent.[29] In general, the wet-impregnation synthesis method usually entails an average use of 20 mL of solvent (commonly methanol) per gram of porous support. It is well-known that methanol is highly toxic and exhibits a huge carbon footprint, around 160 $g_{CO_{2eq}}$/MJ and 93−97 $g_{CO_{2eq}}$/MJ when produced from coal and natural gas, respectively.[30] Although several one-pot sorbent synthesis methods have been reported for obtaining sorbents for CO_2 capture, solvent-minimized synthesis methods for amine-based

https://doi.org/10.1021/acsomega.4c05639
ACS Omega 2024, 9, 45970−45982

sorbents are scarcely reported.[31−33] It is highly desirable to develop novel material synthesis methods, minimizing the use of toxic and volatile solvents to minimize the carbon footprint of DAC materials. Additionally, most studies that have analyzed amine degradation used CO_2 in inert gases (e.g., He, Ar, or N_2) and used TGA and/or DSC and/or TGA-DSC to measure sorbent performance, which does not simulate realistic DAC conditions. To the authors' knowledge, no study has developed a comprehensive accelerated testing (AT) protocol to elucidate sorbent long-term stability and performance under realistic DAC conditions. The aim of this work is to (I) develop a solvent-minimized synthesis method for PEI-silica powder and subsequent pelletization of the sorbent powder and (II) develop an AT protocol mimicking DAC conditions to determine sorbent long-term stability at 80, 100, and 120 °C regeneration temperatures in three different environments: (case I) 21% oxygen-containing environment (ambient air), (case II) purge gas (N_2), and (case III) sorbent saturated with dry and humid CO_2 in an O_2-free environment. A comprehensive understanding of PEI-sorbent degradation in environments relevant to the DAC of CO_2 process conditions would guide advanced material design and efficient process development to improve sorbent lifetime.

2. RESULTS AND DISCUSSION

2.1. Physical and Chemical Properties of PEI-Silica Sorbents. FTIR was used to evaluate the incorporation of PEI onto silica matrices (powder and pellets), as shown in Figure 1a. The spectra for silica powder (blue) showed an intense peak at 1100 cm^{-1}, which is associated with asymmetric Si−O−Si stretching vibrations. The Si−O−Si peak at 1100 cm^{-1} is observed in the PEI-silica powder and pellets. The differences between pristine silica and the PEI-based sorbent (powder and pellets) are the absorption bands near 1450 and 2900 cm^{-1} (highlighted regions), which are attributed to C−H deformation and stretching, respectively. The peaks at ca. 1600 and 3285 cm^{-1} are associated with asymmetric and symmetric N−H stretching of secondary amines, respectively, confirming the successful loading of PEI onto the silica matrix. A noticeable peak at ca. 3600 cm^{-1} in the PEI-silica pellets could be due to the −OH stretching band of bentonite clay, which is in agreement with previously reported literature.[34]

TGA experiments were conducted to estimate the amount of amine incorporated into the silica matrix, as shown in Figure 1b. Sorbent samples (5−10 mg) were loaded into a TGA pan, and the temperature was ramped from RT to 1000 °C at a heating rate of 2.5 °C/min under N_2 flow (200 cc/min). As seen in Figure 1b, the weight loss of silica powder was found to be only 2.5%, whereas the weight loss measured for the PEI-silica powder and pellets was 52.5 and 47.5%, respectively. The weight losses of 2.30 and 7.10% for PEI-silica powder and PEI-silica pellets, respectively, before reaching 120 °C are attributed to the desorption of the preadsorbed components (e.g., moisture and CO_2) from handling in an ambient atmosphere. The prominent derivative peaks at ∼300 °C for PEI-silica powder and at ∼250 and ∼300 °C for PEI-silica pellets, resulting from the loss of PEI, provide evidence of the successful incorporation of PEI into the silica matrix. The second derivative peak in the PEI-silica pellets can be attributed to the 5% weight loss of the MC (organic binder) used for pellet formation. Thus, the estimated weight percentage of aminopolymer (i.e., amine loading) in the synthesized PEI-silica powder and pellets, as measured via TGA weight loss curves, is ca. 50.2 and 39.2%, respectively. These values are near the targeted proportions of amine incorporation (50 and 40%) during the sorbent synthesis process.

Scanning electron microscopy (SEM) micrographs of the pristine silica and PEI-based sorbents, both powder and pellets, were taken to realize the surface morphology of the sorbent, as shown in Figure 2a−c. SEM micrographs reveal no clear

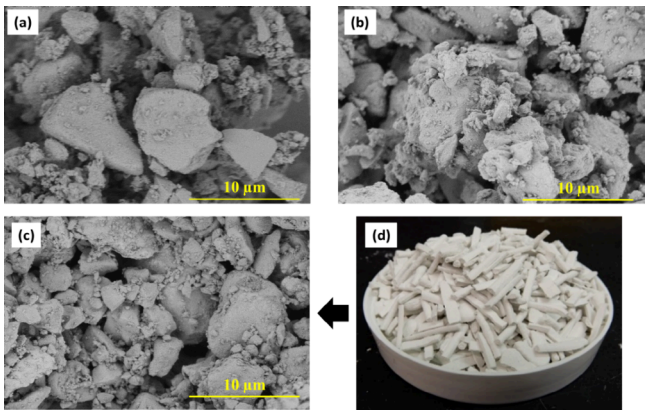

Figure 2. SEM micrographs of silica powder (a), PEI-silica powder (b), PEI-silica pellets (c), and PEI-silica pellets (d).

morphological differences between PEI-silica powder and PEI-silica pellets. The silica powder (Figure 2a) reveals a very open structure, whereas the PEI-silica powder (Figure 2b) and PEI-silica pellets (Figure 3c) appear to be progressively more cluttered. The porous structure of pristine silica and PEI-loaded samples with particle sizes between 2 and 7 μm is shown in Figure 2a−c, whereas Figure 2d displays the as-printed PEI-silica pellets. The average as-printed pellets were 1.64 ± 0.08 cm long, 0.30 ± 0.03 cm wide, and 0.26 ± 0.02 cm high, as shown in Figure S1a.

The N_2 physisorption isotherms and the physical properties of pristine silica, PEI-silica powder, and PEI-silica pellets are shown in Figure 3 and Table 2, respectively. Figure 3 depicts a typical type IV isotherm with an H-1 hysteresis loop for the base silica support, consistent with its mesoporous structure. As expected, the PEI-silica powder and pellets (Figure 3b) exhibited drastically lower N_2 uptake than pristine silica (Figure 3a), correlating with their lower surface areas of 5 and 10 m^2/g, respectively, when compared to the pristine silica powder with 302 m^2/g. This is attributed to aminopolymer loading, reducing the total possible sorption sites for N_2. A slightly higher surface area (S_{BET}, Table 2) for PEI-silica pellets was observed when compared to the powder counterpart, which could be associated with additives (BC-26 m^2/g) used in pellet formation. The same trend was also observed in pore volume (Table 2), where the measured pore volumes of PEI-silica powder and pellets (0.04 and 0.07 cm^3/g, respectively) were more than an order of magnitude lower than the pore volume of pristine silica (1.06 cm^3/g). The calculated pore width for silica, PEI-silica powder, and PEI-silica pellets were 14, 28, and 28 nm, respectively. The physical and chemical properties of the solvent-minimized PEI-silica powder and PEI-silica pellets, fabricated using 94% lower amounts of volatile and toxic methanol solvent, are in close agreement with traditionally synthesized PEI-based sorbents, as compared and shown in Table 3.[18,34−37] Herein, for the rest of the discussion,

https://doi.org/10.1021/acsomega.4c05639
ACS Omega 2024, 9, 45970−45982

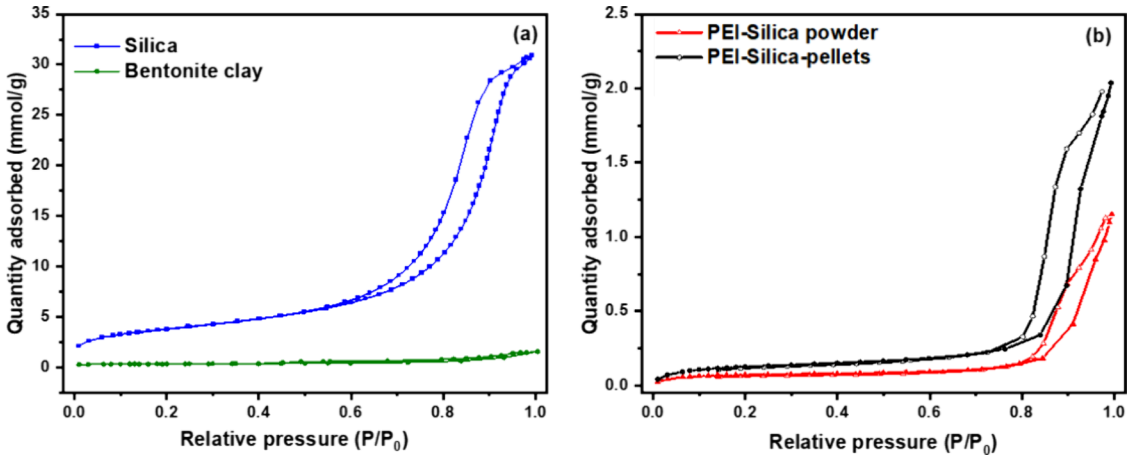

Figure 3. N_2 physisorption isotherms of (a) mesoporous silica and bentonite clay and (b) synthesized PEI-silica powder and PEI-silica pellets.

Table 2. Measured Physical Properties of Sorbent Materials

sorbent	surface area, S_{BET} (m^2/g)	pore volume (cm^3/g)
silica powder	302	1.06
bentonite clay	26	0.04
PEI-silica powder	5	0.04
PEI-silica pellets	10	0.07

PEI-silica pellets are of primary interest for CO_2 sorption and sorbent degradation analysis.

Table 3. Comparison of the Textural Properties of Traditionally Fabricated PEI-Based Sorbents and PEI-Silica Pellets Fabricated in This Study Using a Solvent-Minimized (ca. 94%) Centrifugal Mixing Method

sorbent material	methanol/support (g/g)	amine loading (wt %)	Surface area, S_{BET} (m^2/g)	pore volume (cm^3/g)	ref
PEI-alumina powder	30	32	29	0.27	18
PEI-silica powder	18.3	33	122	0.56	36
PEI-silica powder	15.8	41	100	0.53	
PEI on G-10 silica powder	10	40	65	0.44	35
PEI on G-10 silica powder		50	33	0.25	
PEI-alumina powder	73.1	30	16	0.08	37
PEI-silica powder	15.8	50	22	0.13	34
PEI-silica monolith		40	12	0.03	
PEI-silica powder	0	~50	5	0.04	this work
PEI-silica pellets	0.475	~40	10	0.07	

2.2. CO_2 Sorption and Sorbent Degradation Analysis.

2.2.1. TGA Analysis. Analysis of five temperature swing adsorption−desorption cycles was carried out on PEI-silica pellets to measure and assess their CO_2 adsorption capacity under DAC conditions, as well as sorbent degradation under N_2 purge at 80, 100, and 120 °C using TGA, as shown in Figure 4. Additionally, the CO_2 uptake of pristine silica, PEI-silica powder, and pellets at room temperature is shown in Figure S2. Figure 4A illustrates that the PEI-silica pellets exhibit CO_2 adsorption capacities of around 1 mmol/g (cycle 1) when measured in TGA with 420 ppm of CO_2 as compared to pristine silica (0.15 mmol/g). The PEI-silica pellets showed ~11% lower CO_2 adsorption capacity compared to the PEI-silica powder (Figure S2), which could be attributed to the lower estimated PEI content (39.2 vs 50.2 wt %) in the pellet form as compared to powder form due to the presence of additives used in formulating the sorbent pellets. The adsorption capacities of the solvent-minimized PEI-silica powder and pellets, synthesized using 94% less solvent, are in close agreement with the PEI-based solid sorbents synthesized using the traditional wet-impregnation method, as compared and shown in Table 4.[18,20,21] This shows that centrifugal mixing is an effective method for loading PEI into the mesoporous inorganic support. The sorbent deactivation rates measured for PEI-Silica pellets are reported in Figure 4b. When comparing the fifth temperature swing cycle to the pristine material, the sorbent degraded by ca. 2.7, 4.6, and 9.7% at 80, 100, and 120 °C, respectively. This degradation should be attributed to purely thermal degradation, as residual oxygen was removed by purging with N_2 before desorption at elevated temperatures.

2.2.2. Chemisorption Analysis. Sorption analysis was carried out on PEI-silica pellets and pristine silica powder at three different temperatures (5, 15, and 25 °C) using a 3Flex Adsorption Analyzer (Micromeritics, Norcross GA) in chemisorption mode, as shown in Figure S3. Analysis of PEI-silica powder was not included, as the sorption analysis mainly focused on PEI-silica pellets. As expected, the physisorption of pristine silica showed a higher CO_2 adsorption capacity at lower temperatures. The measured CO_2 adsorption capacities of pristine silica were 0.021, 0.020, and 0.016 mmol/g at 5, 15, and 25 °C, respectively (Figure S3, filled symbols) at 420 ppm (0.042 bar). Unlike pristine silica, the measured CO_2 uptake of PEI-silica pellets by chemisorption (Figure S3, empty symbols) was found to be 0.25, 0.83, and 1.04 mmol/g at 5, 15, and 25 °C, respectively, at 0.042 bar (~420 ppm of CO_2), whereas a small increase in CO_2 adsorption capacity (0.35, 0.89, and 1.1 mmol/g) was observed at 1 bar for all three temperatures. The CO_2 uptake of PEI-silica pellets measured using chemisorption aligns closely with the measured TGA uptake (Figure 4a).

2.2.3. Fixed-Bed Breakthrough (BT) Adsorption and Desorption Analysis. Dynamic CO_2 sorption performance of

https://doi.org/10.1021/acsomega.4c05639
ACS Omega 2024, 9, 45970−45982

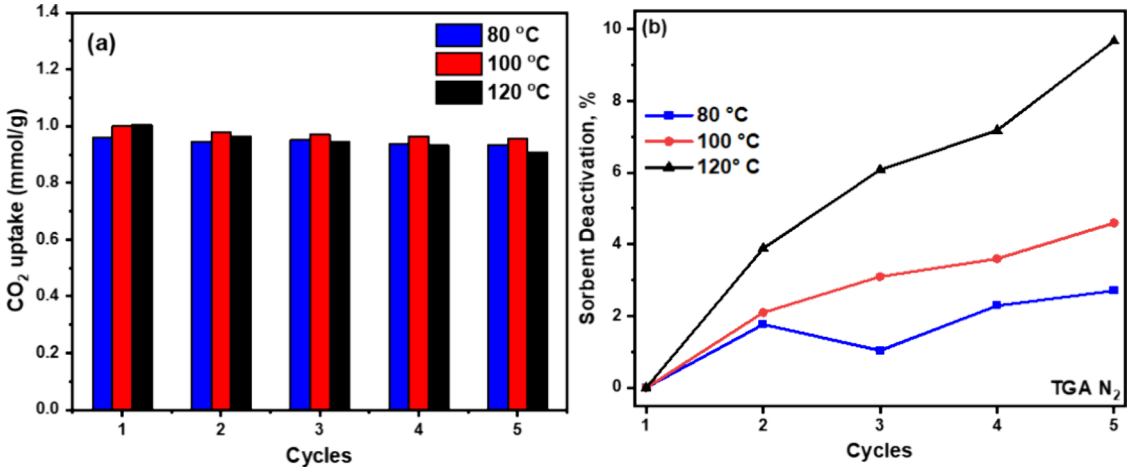

Figure 4. Five cyclic TGA adsorption capacities of PEI-silica pellets at 420 ppm of CO_2 at (a) 25 °C and (b) percent sorbent deactivation.

Table 4. CO_2 Uptake Comparison between Traditionally Fabricated PEI-Based Sorbents and PEI-Silica Pellets Fabricated in This Study Using a Solvent-Minimized (ca. 94%) Centrifugal Mixing Method

sorbent type	methanol/support (g/g)	amine loading (wt %)	adsorbate	CO_2 uptake (mmol/g)	ref
PEI-MIL-101 (Cr) powder	49	30	400 ppm of CO_2, bal. He	0.78	21
	42	50		1.64	
TEPA-MIL-101 (Cr) powder	49	30		1.12	
	42	50		1.26	
PEI-alumina powder	30	32	400 ppm of CO_2, bal. He	1.05	18
PEI-silica powder	19.8	50	400 ppm of CO_2, bal. N_2	1.04	20
PEI-silica powder	0	~50	420 ppm of CO_2, bal. air	1.22	this work
PEI-silica pellets	0.475	~40		1.04	

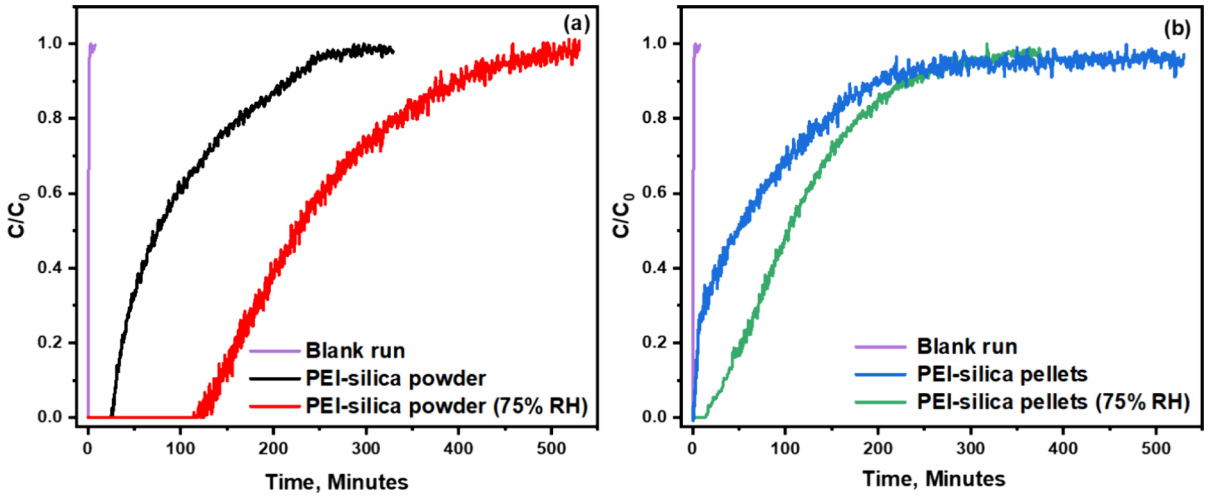

Figure 5. Breakthrough curves under dry and humid (75% RH) conditions of (a) PEI-silica powder and (b) pellets.

the PEI-silica sorbent (powder and pellets) was evaluated using a BT system at ambient conditions (room temperature and atmospheric pressure of about 0.78 bar at Los Alamos, New Mexico, U.S.A). For degradation analysis in a compact fixed-bed sorption column, the pellets were cut lengthwise, as shown in Figure S1b, to reduce the length to 0.37 cm ±0.04 for better packing. The BT curves of the sorbent (both powder and pellets) under dry and humid conditions are depicted in Figure 5. The average humidity (75% RH) of the U.S. was considered to assess sorbent CO_2 uptake performance.[38] As expected, in both cases (powder and pellets), the BT curves in the dry conditions are sharper when compared to humid conditions due to the well-known promoting effect of water vapor on CO_2 adsorption.[15,39] The calculated BT and pseudoequilibrium capacities of both the powder and pellets in dry and humid conditions, as well as the corresponding amine efficiencies, are summarized in Table 5. The pseudo equilibrium BT capacity (at $C/C_o = 0.95$) of PEI-silica powder was found to be 1.25 and 1.9 mmol CO_2/g (Figure 5a), whereas CO_2 uptake for pellets was 1.05 and 1.43 mmol, CO_2/g (Figure 5b) in dry and humid conditions, respectively. The pellets showed relatively less CO_2 uptake in both dry and humid conditions as compared to in the powder form, which can be associated with additives present in the pellets. Based

https://doi.org/10.1021/acsomega.4c05639
ACS Omega 2024, 9, 45970−45982

Table 5. Dynamic Adsorption Performance and Amine Efficiency of the PEI-Silica Powder and Pellets under Dry and Wet (75% RH) Conditions

	pseudoequilibrium capacity ($mmol_{CO_2}/g_{sorbent}$)		amine efficiency (mol_{CO_2}/mol_N)	
sample	dry	wet	dry	wet
PEI-silica powder	1.30	1.95	0.11	0.16
PEI-silica pellets	1.05	1.43	0.10	0.15

on the BT CO_2 uptake and amine loading (wt %) estimated by TGA, the calculated amine efficiency was 45−50% higher for PEI-silica powder and pellets in wet conditions as compared to dry conditions. This dynamic adsorption analysis showed a similar CO_2 adsorption performance and amine efficiency between the solvent-minimized sorbents and sorbents fabricated using traditional wet-impregnation synthesis methods.

To determine desorption efficiency and verify the impact of desorption temperatures (80, 100, and 120 °C) on the adsorption performance of the sorbent, real-time CO_2 concentration measurements were conducted and recorded using a Vaisala CO_2 sensor (GMP 252). The desorption profiles at each desorption temperature with N_2 purge are shown in Figure 6. The desorption areas (area under the desorption curve) at 80, 100, and 120 °C desorption temperatures were measured to be 38,655; 49,243; and 81,128 (arbitrary units), respectively. The corresponding desorption area calculated for CO_2 desorption curves at 80 and 100 °C is 52.35 and 39.30% lower than that calculated for the desorption curve at 120 °C. As shown in Figure 6, desorption times for 80, 100, and 120 °C were found to be 3, 1, and 2 h, respectively. The higher desorption time required for 120 °C is due to the relatively lower heating rate (∼2.3 °C/min) when compared to 80 and 100 °C, (Figure 6). Assuming the same heating times (i.e., ∼15 min ramp to desired regeneration temperature), desorption times should be 3, 1, and 1 h for 80, 100, and 120 °C, respectively. Thus, this desorption analysis demonstrates that the heating rate and temperature are extremely important in achieving efficient desorption for DAC.

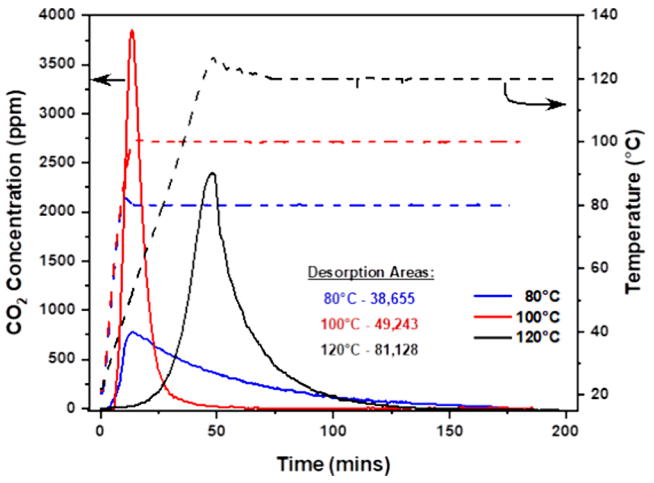

Figure 6. CO_2 desorption and temperature profiles of the PEI-silica pellets at regeneration temperatures of 80, 100, and 120 °C.

2.3. Accelerated Testing (AT) Analysis. Accelerated testing (AT) of structured sorbents (PEI-silica pellets) was performed to hasten time-consuming cyclic processes and quantitatively realize the sorbent's long-term degradation behavior. In AT, PEI-silica pellets were exposed to a desired regeneration temperature for 24 and 100 h under four distinct environments representative of the DAC of CO_2 process conditions: case I: ambient 21% oxygen-containing (O_2) environment; case II: pure N_2 environment; and case III: sorbent saturated with dry and humid (75% RH) CO_2 in an oxygen-free environment. AT was performed for 24 h (case I) and 100 h (cases II and III) at 80, 100, and 120 °C using the conditions outlined in Section 4.4 with the same temperature profiles shown in Figure S4. Assuming the same heating time for desorption as described in Section 2.2.3, 24 h AT correlates to 8, 24, and 24 adsorption−desorption cycles, whereas 100 h AT corresponds to roughly 33, 100, and 100 cycles for 80, 100, and 120 °C, respectively. The degradation of fresh and post-AT PEI-silica pellets at 80, 100, and 120 °C with N_2 purge using TGA and BT was examined and compared. Moreover, dry and humid CO_2-induced degradation (sorbent saturated with dry and humid CO_2) was performed on BT in an oxygen-free environment at the same regeneration temperatures. An FTIR analysis was carried out on post-AT (24 and 100 h) samples to assess and verify sorbent degradation.

2.3.1. 24 h AT (21% O_2). Sorbent deactivation analysis was performed on PEI-silica pellets for 24 h under ambient air (21% O_2 environment (case I)), with the corresponding FTIR spectra displayed in Figure 7. As shown in Figure 7a, post-AT

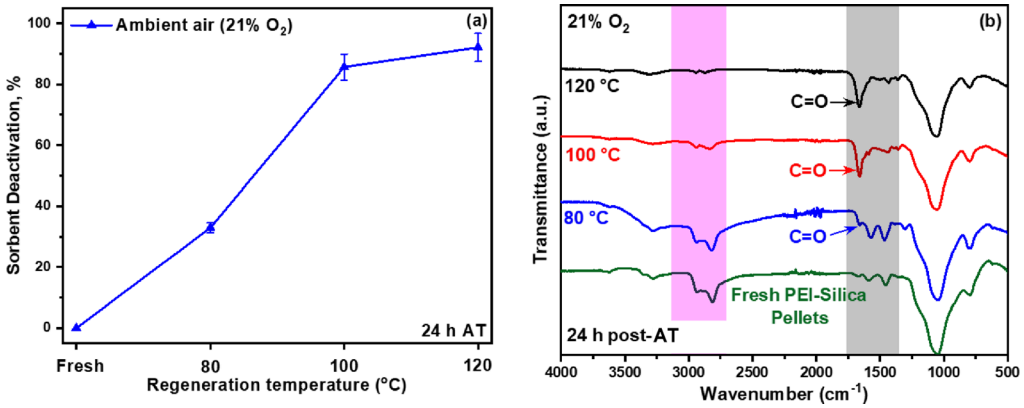

Figure 7. Analysis of post-AT PEI-silica pellets at 80, 100, and 120 °C regeneration temperatures with (a) sorbent deactivation of 24 h AT experiments in ambient air (21% O_2) and (b) FTIR spectra of post-24 h AT experiments used with a 21% O_2.

https://doi.org/10.1021/acsomega.4c05639
ACS Omega 2024, 9, 45970−45982

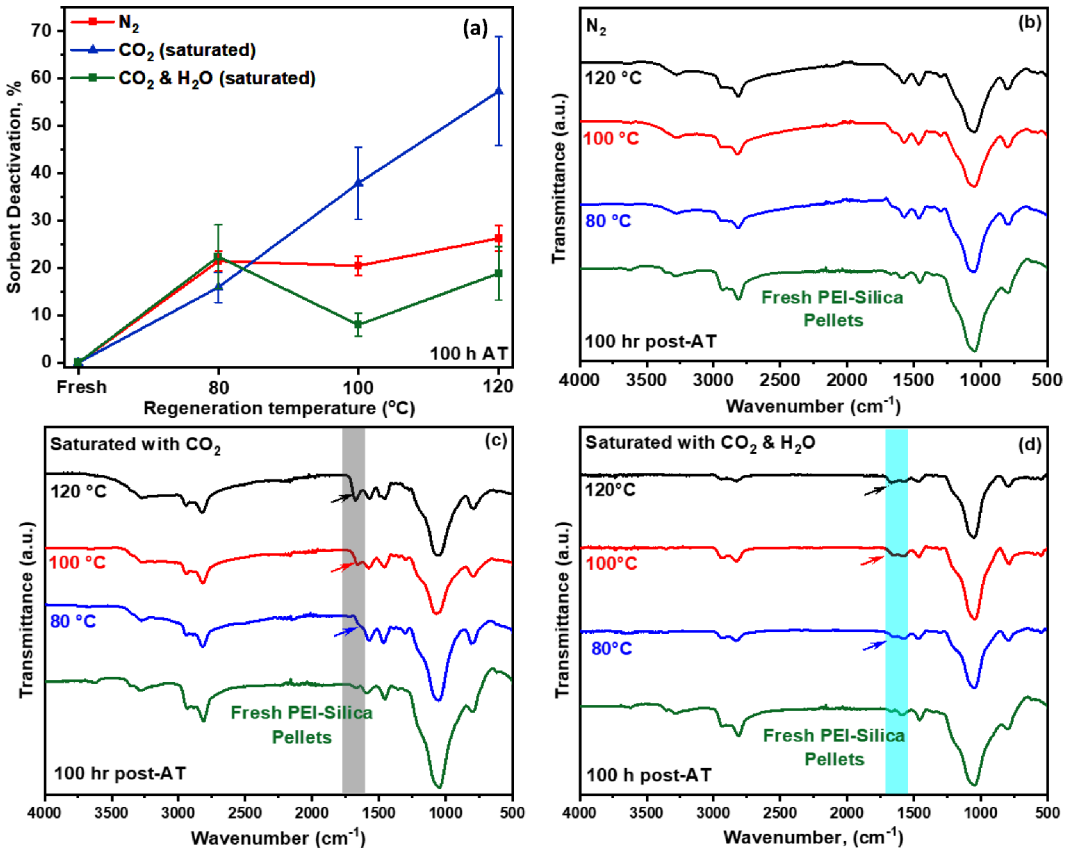

Figure 8. Analysis of fresh and post-AT PEI-silica pellets at 80, 100, and 120 °C regeneration temperatures with (a) sorbent deactivation of all 100 h AT experiments for all three cases, (b) FTIR spectra of post-AT samples used with a N_2 environment, FTIR spectra of post-AT saturated (c) dry, and (d) wet (75% RH) CO_2 samples.

BT PEI-silica pellets showed substantial degradation of ca. 33.0, 85.7, and 92.1% at 80, 100, and 120 °C, respectively. The sorbent degradation increased dramatically from 80 to 100 °C (>50%), revealing a facilitated aerobic reaction with PEI at temperatures ≥80 °C. The degradation is visually observed in post-AT samples based on their discoloration (Figure S5). The oxidative degradation was further verified by the FTIR spectra carried out on post-AT BT samples, as shown in Figure 7b. The FTIR spectra revealed the development of a carbonyl (C═O) band at 1660 cm^{-1} in post-AT samples at all three temperatures.[18] It is also important to note that the intensity of the carbonyl (C═O) band in the FTIR spectra (Figure 7b, gray highlighted region and denoted by arrows) is directly proportional to the temperature (80 < 100 < 120 °C). The development of this bond corresponds to a decrease in the CO_2 capture capacity, affirming the degradation effect of O_2 at elevated temperatures. Moreover, the loss of the C−H vibrational stretching band at ∼2900 cm^{-1} (pink highlighted region) and N−H band at ∼1400 cm^{-1} with an increase in temperature (80 < 100 < 120 °C) indicates the transformation of C−H and N−H to C═O due to the reaction of oxygen with PEI at elevated temperatures.

2.3.2. 100 h AT (N_2, CO_2, and CO_2 + H_2O). 100 h AT (equivalent to 33, 100, and 100 cycles) was performed on the fixed-bed (BT) column with N_2, CO_2, and CO_2 and H_2O environments as a function of regeneration temperatures of 80, 100, and 120 °C, and their corresponding post-AT analyses are displayed in Figure 8. The 100 h AT on BT (Figure 8a) under the N_2 environment (case II) showed that the adsorption capacity of PEI-silica pellets dropped by ca. 21.1, 20.5, and 26.2% with increasing regeneration temperatures. FTIR spectra of 100 h AT under N_2 carried out on the post-AT sorbent samples showed that the sorbent largely retained its chemical bonds even after its exposure to all three regeneration temperatures for 100 h continuously, as depicted in Figure 8b. Thus, it can be concluded that the sorbent is relatively stable under the N_2 environment with a moderate loss (20−26%) in its capture performance depending on the regeneration temperature. The loss in capacity observed can be attributed to the loss of amines via amine evaporation, which is attributed to elevated temperatures during regeneration.[15] 100 h AT with 21% O_2 on PEI-silica pellets was not performed as the sorbent substantially degraded (up to 94%), as observed in the 24 h AT (Figure 7).

To measure dry and wet (75% RH) CO_2-induced degradation and determine sorbent stability, sorbents saturated with dry and wet CO_2 were exposed to all three regeneration temperatures for 100 h (equivalent to 33, 100, and 100 cycles) continuously in an oxygen-free environment in the fixed-bed BT column. The corresponding sorbent deactivation and FTIR spectra are shown in Figure 8. Previously, Heydari et al. investigated CO_2-driven amine sorbent degradation by exposing the sorbent to 5% CO_2 balanced in N_2 for 10 h at 85, 105, and 120 °C. They concluded that the sorbent lost 2, 25, and 68% of its capture capacity, respectively.[15] Another study concluded that PEI-based sorbent degradation was aggravated by ∼2× due to the presence of water vapor in aerobic environments.[18] However, the degradation based on

https://doi.org/10.1021/acsomega.4c05639
ACS Omega 2024, 9, 45970−45982

5% CO_2 in N_2 and the aerobic environment in DAC due to vacuum (to remove oxygen) does not simulate realistic industrial DAC conditions, where CO_2 degradation usually occurs based on sorbents saturated with dry or wet CO_2. Thus, the protocol (Section 4.4, case II) established in this study was to better mimic industrial DAC conditions and measure realistic CO_2-induced degradation. As can be seen in (Figure 8a), the measured dry CO_2-induced degradation after 100 h is ca. 15.7, 37.9, and 57.3% at increasing regeneration temperatures of 80, 100, and 120 °C. As expected, CO_2-induced degradation was found to be 17.5 and 31.0% higher at 100 and 120 °C, respectively, when compared to N_2 purge degradation. It is worth noting that the CO_2-induced degradation at the lowest regeneration temperature (80 °C) was similar to the degradation under inert (N_2) atmosphere. Post-AT, the 100 h dry CO_2-induced degradation was additionally characterized via FTIR, as depicted in Figure 8c. The FTIR spectra unveiled the development of a slight band at 1660 cm^{-1} (shown by an arrow and in the gray highlighted region) at 80 °C, whereas prominent bands (1660 cm^{-1}) at 100 and 120 °C could be attributed to NH_2 deformation of hydrogen-bonded amino groups and the formation of open chain urea (NH_2CONH_2), respectively, in agreement with previously reported investigations.[15,18,36,40] The intensity of the band at 1660 cm^{-1} is directly proportional to the regeneration temperatures (80 < 100 < 120 °C), indicating a stronger reaction of CO_2 with aminopolymer groups at higher temperatures. It is also important to note that the C−H vibrational stretching band at ∼2900 cm^{-1} was found to be unchanged at all three regeneration temperatures as opposed to case I (21% O_2), verifying open chain urea formation.

On the other hand, the 100 h AT analysis on the sorbent saturated with wet CO_2 (case III) showed 30−40% and ca. 10% higher stability compared to saturated CO_2 (dry) and N_2 environments, respectively. The higher stability sorbent under wet CO_2 could be associated with stronger interactions between H_2O and PEI, inhibiting urea formation and decelerating degradation as compared to dry CO_2-induced degradation.[17,41] Sorbent degradation was found to be higher at 80 °C compared to 100 and 120 °C, which could be attributed to lower regeneration efficiency at lower temperatures, as shown in Figure 6. Post-100 h AT of wet CO_2-induced degradation was characterized by FTIR, as depicted in Figure 8d. The FTIR results revealed the disappearance of a band at ∼3285 cm^{-1} (N−H stretching band) and the development of a convoluted peak at ∼1660 cm^{-1} (shown by an arrow and in the blue highlighted region), which could be associated with the formation of ammonium carbamate or bicarbonate, closely aligning with previously reported results.[39] This wet CO_2-induced AT degradation analysis suggests an important role of water vapor in alleviating sorbent degradation. An abridged summary of the PEI degradation mechanisms under (a) O_2 and (b) CO_2, based on previous studies, is depicted in Figure S6.

Table 6 compares the degradation of PEI-silica pellets based on AT in four different environments at 80, 100, and 120 °C. In 100 h AT, sorbent deactivation under N_2 purge and wet CO_2 environments was found to be slightly higher at 80 °C when compared to 100 and 120 °C. This could be attributed to either inefficient regeneration (Figure 6) or the readsorption of CO_2, which is supported by previous studies that have demonstrated that PEI-silica adsorbents exhibit higher CO_2 adsorption capacities at ∼75 °C than at room temperature due to improved diffusional (CO_2 diffusion and PEI chain mobility) effects.[34,36] Interestingly, 100 h AT under a wet CO_2 environment showed the highest stability among all environments, indicating that humidity greatly hinders urea formation. AT experiments for all three cases showed the highest degradation at 120 °C, making this regeneration temperature undesirable for DAC with PEI-based sorbents. Based on overall degradation, the optimum regeneration temperature was found to be in the range of 80 < $T \leq$ 100 °C.

Table 6. Summary of Overall PEI-Silica Pellet Degradation Evaluation Performed at 80, 100, and 120 °C in Various Regeneration Environments

experiment	regeneration temperature (°C)	degradation (%)
	Case I: Ambient Air (21% O_2)	
24 h AT	80	32.93
	100	85.67
	120	92.10
	Case II: N_2	
100 h AT	80	21.41
	100	20.46
	120	26.25
	Case III: Dry Saturated CO_2	
100 h AT	80	15.90
	100	37.89
	120	57.28
	Case III: Wet Saturated CO_2 (75% RH)	
100 h AT	80	20.22
	100	7.96
	120	18.84

3. CONCLUSIONS

A novel solvent-minimized method of synthesizing PEI-silica sorbents via centrifugal mixing was developed, enabling PEI-silica pellet fabrication using ca. 94% lower amounts of volatile and toxic solvent for the DAC of CO_2. The sorbent was extensively evaluated to benchmark its CO_2 capture performance, and AT protocols were developed to assess the long-term degradation of the sorbent in environmental conditions representative of industrial DAC processes. BT cyclic experiments with N_2 purge indicated that the sorbent showed quite stable performance and low degradation at 120 °C regeneration temperatures, whereas incomplete desorption at 80 °C resulted in lower CO_2 working capacities. Conversely, TGA cyclic runs with N_2 purge showed that sorbent degradation is linear and directly proportional to the regeneration temperatures (120 > 100 > 80 °C). The BT cyclic runs with ambient air (21% O_2) showed substantial degradation (up to 94% within 24 h at 120 °C) due to the aerobic oxidation of amines at elevated regeneration temperatures, as evident by the FTIR spectra showing the development of C═O bonds from C−H and N−H bonds. 100 h AT analysis showed that CO_2-induced sorbent degradation (case III) via urea formation was 2−3x higher at elevated regeneration temperatures (≥100 °C) than the sorbent degradation in inert N_2 (case II) or CO_2-induced degradation at lower (80 °C) temperatures. In the presence of 75% RH, the PEI-silica sorbent is shown to be less prone to degradation, which is attributed to the suppression of urea formation by favorable interactions between water vapor and the N−H groups of PEI molecules. Based on the analysis of

https://doi.org/10.1021/acsomega.4c05639
ACS Omega 2024, 9, 45970−45982

AT results, the optimum regeneration temperature for the PEI-based sorbents is determined to be between 80 and 100 °C.

4. MATERIALS AND EXPERIMENTAL METHODS

4.1. Materials. Mesoporous silica (PD-09024, Ecovyst, Inc.) was used to synthesize the PEI-silica powder and pellets. Bentonite clay (BC) binder, methyl cellulose (MC) plasticizer, PEI (800 M_w), and methanol were all obtained from Sigma-Aldrich. All materials were used with no prior treatment. For gas analysis, 420 ppm of CO_2 balanced in air (contains 21% O_2) and ultrahigh purity N_2, all obtained from Airgas, were used for adsorption and desorption, respectively.

4.2. Preparation of PEI-Silica Powder and Pellets. High-speed centrifugal mixing (THINKY ARE-250) was used to synthesize solvent-minimized PEI-impregnated silica powder. Briefly, mesoporous silica (10.0 g) was outgassed at 120 °C under vacuum for 12 h. Then, PEI (10.0 g) and the degassed silica were loaded into a THINKY centrifugal cup, mixed for 5 min, and defoamed for 1 min at 2000 rpm. The PEI-silica powder was then dried for 12 h at 100 °C in ambient air. This resulted in PEI-silica powder with a 50% PEI loading, which has previously been shown to be optimal for uniform distribution on mesoporous silica supports.[42]

For PEI-silica pellet synthesis, PEI-silica powder (12.0 g) and methanol (9.50 g) were loaded into a THINKY cup, and a powder mixture of binder (BC, 2.25 g) and plasticizer (MC, 0.750 g) was added (i.e., 20 wt % additives). The binder adheres to the PEI-silica particles, while the plasticizer adheres to the PEI-silica/binder particles, leading to mechanically strong pellet formation. This composition was then mixed in the THINKY mixer with the same conditions used in the formulation of PEI-silica powder to obtain a homogeneous slurry for 3D-printing. 3D-printing has proven to be a promising method for processing various sorbents into structured configurations (i.e., monoliths).[34,43,44] The slurry was loaded into a 30 cc syringe, and compressed air was used to dispense the slurry onto the print bed to print pellets, which can be seen in Figure 9. The pellet configuration is considered

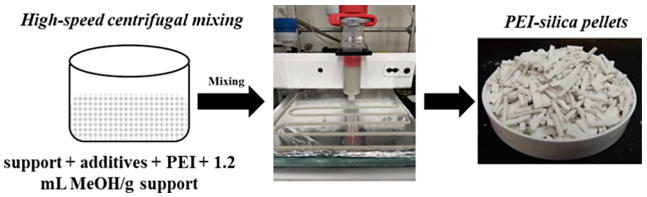

Figure 9. Preparation of PEI-silica pellets using the 3D-printing technique.

as a structured form which can be directly deployed for large-scale DAC. The printed pellet geometry was cut into similar sized pieces to form pellets, followed by curing the pellets at 100 °C for 12 h. From this process, pellets with 20 wt % additives and an 80% PEI-silica loading with a 1:1 PEI to silica ratio (i.e., 40 wt % PEI and 40 wt % silica) were obtained and used for all experiments. Compared to conventional synthesis methods of fabricating PEI-silica sorbents that use ca. 20 mL of solvent per gram of support, this method utilized 94% less toxic and volatile methanol solvent.[31−33]

4.3. Characterization of PEI-Silica Powder and Pellets. Fourier transform infrared (FTIR) spectroscopy was performed on a Nicolet iS50 spectrometer with an attenuated total reflectance (ATR) module using a diamond crystal, a Polaris High Stability source, and a DLaTGS detector. Powder samples were placed directly onto the ATR instrument for measurement. Spectra were collected from 500 to 4000 cm^{-1} with a resolution of 4 cm^{-1}. All IR data presented were not signal-averaged and are presented with baseline correction.

Thermogravimetric analysis (STA-650; Hitachi) was used to estimate the PEI loading in PEI-based sorbents (powder and pellets). The sorbent was heated to 1000 °C at a heating rate of 2.5 °C min^{-1} under a 200 cc/min N_2 flow to evaporate or degrade all pellet constituents other than silica.

SEM was used to characterize the sorbent morphology. The base silica support, PEI-impregnated silica, and formed pellets were prepared for analysis by attaching each sample to a SEM stub using carbon tape. The samples were then sputtered with approximately 5 nm of gold and placed on a multisample stage of a Thermo Apreo 2 SEM. The samples were analyzed using electron beam settings of 5 kV and 6.3 pA.

N_2 physisorption measurements were performed by using a 3Flex Adsorption Analyzer (Micromeritics, Norcross GA). Samples were degassed in an external drying oven (Binder Gmbh, Germany) at 105 °C under nitrogen for 3 h before being transferred into the adsorption analyzer, at which point vacuum was applied for 30 min prior to analysis. N_2 sorption was conducted at liquid nitrogen (LN_2) temperature, −196 °C (77K), with P_{sat} being measured at each point. Approximately 27 adsorption points and 20 desorption points were taken at pressures between P/P_o of 0.01 and 0.99. The BET surface area method was used to determine the sample surface area by a linear fit of the adsorption data between P/P_o of 0.05 and 0.3. The pore volume was determined at P/P_o = 0.99, and the average pore diameter was obtained using D = 4 V/A with the BET method, where D is the cylindrical pore diameter, V is the pore volume, and A is the pore area.

4.4. CO_2 Sorption Analysis. CO_2 sorption analysis was carried out at 0.78 bar (atmospheric pressure at Los Alamos, NM) and the desired temperature. Thermogravimetric analysis (STA-650; Hitachi) was used for preliminary measurements of the CO_2 uptake capacity of the PEI-silica pellets. Briefly, the sample (5−10 mg) was degassed for 2 h at 120 °C under N_2 (200 cc/min), followed by cooling to room temperature (RT). Then, 420 ppm of CO_2 in air was flowed into the system at 300 cc/min for 250 min.

CO_2 sorption was also measured on a 3Flex Adsorption Analyzer (Micromeritics, Norcross GA) in chemisorption mode. Samples were dosed with 99.999% pure CO_2 under isothermal conditions at pressures between 25 and 550 mmHg. Prior to analysis, samples were degassed in situ by heating to 120 °C for 2 ± 0.5 h under a purge of 99.999% helium (He) at 50 sccm. Isothermal conditions (±0.1 °C) were maintained during analysis using a Micromeritics Iso Controller with water as the conduction fluid.

The schematic of the fixed-bed BT system used to measure the CO_2 capture performance and stability of PEI-silica pelletized sorbents at various temperatures is shown in Figure 10. The weight of the PEI-silica pellet samples was ∼0.2 g for all BT experiments. The N_2 purge flow was set to 200 cc/min because it was found to be the optimal flow rate, as described in Figure S7. For wet CO_2 experiments, a controlled adsorbate flow with a bubbler was utilized to achieve the desired humidity (75% RH). Flow rates to achieve 75% RH were determined by dew point readings of the gas inputs, as measured by a Cermet II Hygrometer (Kahn Instruments).

https://doi.org/10.1021/acsomega.4c05639
ACS Omega 2024, 9, 45970−45982

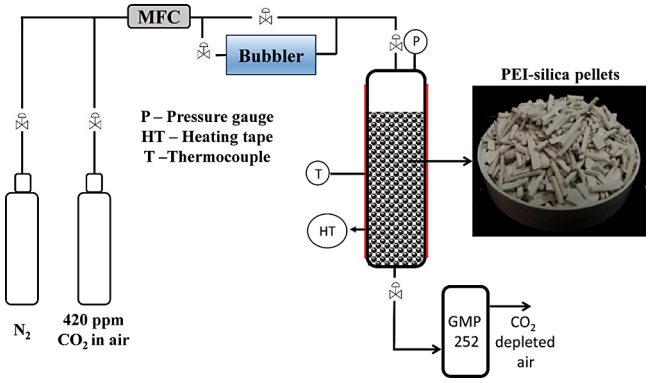

Figure 10. Breakthrough (BT) system flow schematic.

Desorption was performed in the regeneration environment at 80, 100, and 120 °C, with heating rates of ∼8, 10, and 2 °C/min, respectively, due to PID settings of the temperature controller to avoid overshooting the desorption temperature. The adsorption and desorption times for all fixed-bed experiments were set to 250 and 180 min, respectively. A GMP 252 (Vaisala) CO_2 sensor, which exclusively measures CO_2 concentrations in the accurate range of 0−10,000 ppm, was used to measure real-time CO_2 concentrations. The sensor was calibrated at Los Alamos atmospheric pressure of 0.78 bar prior to the experiments using ultrahigh purity N_2 and premixed CO_2/air calibration mixtures (420, 3000, and 5000 ppm of CO_2 balanced in air), all obtained from Airgas.

AT was performed on the sorbent samples via the BT system, where the samples were exposed to 80, 100, and 120 °C. At these temperatures, sorbent degradation was investigated under three different process-relevant environments: (case I) ambient air at 21% O_2, (case II) N_2 purge gas, and (case III) N_2 gas mixed with CO_2 degassed from a saturated sorbent. Case III was investigated under both dry and humid conditions. Twenty-four h AT testing was performed for case I, whereas 100 h AT was performed for cases II and III. AT experimental temperature profiles for cases II and III are shown in Figure S4. Briefly, all samples were degassed at 120 °C under N_2 prior to AT. Then, one adsorption/desorption cycle (C1) was performed using 420 ppm of CO_2 ambient air. This measured the initial CO_2 uptake of the sorbent. For case II, CO_2 was completely purged from the breakthrough column, which established an N_2 environment during testing. For case III, the sorbent was degassed at 120 °C, followed by adsorption and desorption for one cycle to again establish baseline performance. CO_2 adsorption was performed to saturation a second time (C2). The column was then flushed with N_2 at RT to establish an O_2-free environment, and the breakthrough column was isolated. This ensured that the sorbed CO_2 was under a N_2 environment. This process was repeated with humid (75% RH) feed gas. For all cases, the sorbent was heated and held at the desired AT temperature for 100 h at 80 °C (simulating 33 cycles) and for 100 h at 100 and 120 °C (simulating 100 cycles), followed by cooling down to RT and final adsorption (C_{100}). This is further explained in Section 2.3.

■ ASSOCIATED CONTENT

Supporting Information

The Supporting Information is available free of charge at https://pubs.acs.org/doi/10.1021/acsomega.4c05639.

Additional characterization of the sorbents used in this study; photographs of the as-printed, as-used, and post-test sorbents; graphical depictions of the temperature profiles used for accelerated testing; degradation mechanisms of PEI; and optimization of N_2 purge rate during desorption (PDF)

■ AUTHOR INFORMATION

Corresponding Authors

[+]**Harshul V. Thakkar** − *Material Synthesis and Integrated Devices (MPA-11) Group, Material, Physics and Applications Division, Los Alamos National Laboratory, Los Alamos, New Mexico 87545, United States;* orcid.org/0000-0001-7700-1026; Email: hthakkar1126@gmail.com

Rajinder P. Singh − *Material Synthesis and Integrated Devices (MPA-11) Group, Material, Physics and Applications Division, Los Alamos National Laboratory, Los Alamos, New Mexico 87545, United States;* orcid.org/0000-0003-4634-4290; Email: rsingh@lanl.gov

Authors

[+]**Andrew J. Ruba** − *Material Synthesis and Integrated Devices (MPA-11) Group, Material, Physics and Applications Division, Los Alamos National Laboratory, Los Alamos, New Mexico 87545, United States;* orcid.org/0009-0004-6022-8960

John A. Matteson − *Material Synthesis and Integrated Devices (MPA-11) Group, Material, Physics and Applications Division, Los Alamos National Laboratory, Los Alamos, New Mexico 87545, United States*

Michael P. Dugas − *Material Synthesis and Integrated Devices (MPA-11) Group, Material, Physics and Applications Division, Los Alamos National Laboratory, Los Alamos, New Mexico 87545, United States;* orcid.org/0000-0003-4360-5424

Complete contact information is available at: https://pubs.acs.org/10.1021/acsomega.4c05639

Notes

The authors declare no competing financial interest.

[+]H.V.T. and A.J.R. denote equal authorship.

■ ACKNOWLEDGMENTS

The authors acknowledge funding support from LANL Laboratory Directed Research & Development (20230065DR) for this work. The authors would like to thank Rajendra P. Palanisamy for his 3D-prinitng design efforts. The Los Alamos National Laboratory, an affirmative action equal opportunity employer, is managed by Triad National Security, LLC for the U.S. Department of Energy's NNSA, under contract 89233218CNA000001. Any subjective views or opinions that might be expressed in the paper do not necessarily represent the views of the U.S. Department of Energy or the United States Government.

■ REFERENCES

(1) Fu, D.; Davis, M. E. Toward the feasible direct air capture of carbon dioxide with molecular sieves by water management. *Cell Rep. Phys. Sci.* **2023**, *4*, No. 101389.

(2) McQueen, N.; Gomes, K. V.; McCormick, C.; Blumanthal, K.; Pisciotta, M.; Wilcox, J. A review of direct air capture (DAC): scaling up commercial technologies and innovating for the future. *Prog. Energy* **2021**, *3*, No. 032001.

(3) IEA. *Direct Air Capture 2022*; IEA: Paris, 2022.
(4) DOE/EE-2635. *Industrial Decarbonization Roadmap*; United States Department of Energy: 2022.
(5) House, K. Z.; Baclig, A. C.; Ranjan, M.; van Nierop, E. A.; Wilcox, J.; Herzog, H. J. Economic and energetic analysis of capturing CO2 from ambient air. *Proc. Natl. Acad. Sci. U. S. A.* **2011**, *108*, 20428−20433.
(6) Lackner, K. S.; Azarabadi, H. Buying down the Cost of Direct Air Capture. *Ind. Eng. Chem. Res.* **2021**, *60*, 8196−8208.
(7) Stolaroff, J. K.; Baker, S. E.; Peridas, G.; Pang, S. H.; Goldstein, H. M.; Lucci, F. R.; Li, W.; Slessarev, E. W.; Pett-Ridge, J.; Ryerson, F. J.; Wagoner, J. L.; Kirkendall, W.; Aines, R. D.; Sanchez, D. L.; Cabiyo, B.; Baker, J.; McCoy, S.; Uden, S.; Runnebaum, R.; Wilcox, J.; Psarras, P. C.; Pilorgé, H.; McQueen, N.; Maynard, D.; McCormick, C. *Getting to Neutral: Options for Negative Carbon Emissions in California*; Lawrence Livermore National Laboratory, LLNL-TR-796100: 2020.
(8) Sodiq, A.; Abdullatif, Y.; Aissa, B.; Ostovar, A.; Nassar, N.; El-Naas, M.; Amhamed, A. A review on progress made in direct air capture of CO2. *Environ. Technol. Innovation* **2023**, *29*, No. 102991.
(9) Sanz-Perez, E. S.; Murdock, C. R.; Didas, S. A.; Jones, C. W. Direct Capture of CO(2) from Ambient Air. *Chem. Rev.* **2016**, *116*, 11840−11876.
(10) Shi, X.; Xiao, H.; Azarabadi, H.; Song, J.; Wu, X.; Chen, X.; Lackner, K. S. Sorbents for the Direct Capture of CO(2) from Ambient Air. *Angew. Chem., Int. Ed. Engl.* **2020**, *59*, 6984−7006.
(11) Wiegner, J. F.; Grimm, A.; Weimann, L.; Gazzani, M. Optimal Design and Operation of Solid Sorbent Direct Air Capture Processes at Varying Ambient Conditions. *Ind. Eng. Chem. Res.* **2022**, *61*, 12649−12667.
(12) *Negative Emissions Technologies and Reliable Sequestration: A Research Agenda*; National Academies Press: Washington (DC), 2018.
(13) Sinha, A.; Darunte, L. A.; Jones, C. W.; Realff, M. J.; Kawajiri, Y. Systems Design and Economic Analysis of Direct Air Capture of CO2 through Temperature Vacuum Swing Adsorption Using MIL-101(Cr)-PEI-800 and mmen-Mg2(dobpdc) MOF Adsorbents. *Ind. Eng. Chem. Res.* **2017**, *56*, 750−764.
(14) Vohlídal, J. Polymer degradation: a short review, Chemistry Teacher. *International* **2021**, *3*, 213−220.
(15) Heydari-Gorji, A.; Sayari, A. Thermal, Oxidative, and CO2-Induced Degradation of Supported Polyethylenimine Adsorbents. *Ind. Eng. Chem. Res.* **2012**, *51*, 6887−6894.
(16) Rosu, C.; Pang, S. H.; Sujan, A. R.; Sakwa-Novak, M. A.; Ping, E. W.; Jones, C. W. Effect of Extended Aging and Oxidation on Linear Poly(propylenimine)-Mesoporous Silica Composites for CO(2) Capture from Simulated Air and Flue Gas Streams. *ACS Appl. Mater. Interfaces* **2020**, *12*, 38085−38097.
(17) Guta, Y. A.; Carneiro, J.; Li, S.; Innocenti, G.; Pang, S. H.; Sakwa-Novak, M. A.; Sievers, C.; Jones, C. W. Contributions of CO(2), O(2), and H(2)O to the Oxidative Stability of Solid Amine Direct Air Capture Sorbents at Intermediate Temperature. *ACS Appl. Mater. Interfaces* **2023**, *15*, 46790−46802.
(18) Carneiro, J. S. A.; Innocenti, G.; Moon, H. J.; Guta, Y.; Proano, L.; Sievers, C.; Sakwa-Novak, M. A.; Ping, E. W.; Jones, C. W. Insights into the Oxidative Degradation Mechanism of Solid Amine Sorbents for CO(2) Capture from Air: Roles of Atmospheric Water. *Angew. Chem., Int. Ed. Engl.* **2023**, *62*, No. e202302887.
(19) Miao, Y.; He, Z.; Zhu, X.; Izikowitz, D.; Li, J. Operating temperatures affect direct air capture of CO2 in polyamine-loaded mesoporous silica. *Chem. Eng. J.* **2021**, *426*, No. 131875.
(20) Miao, Y.; Wang, Y.; Zhu, X.; Chen, W.; He, Z.; Yu, L.; Li, J. Minimizing the effect of oxygen on supported polyamine for direct air capture. *Sep. Purif. Technol.* **2022**, *298*, No. 121583.
(21) Rim, G.; Kong, F.; Song, M.; Rosu, C.; Priyadarshini, P.; Lively, R. P.; Jones, C. W. Sub-Ambient Temperature Direct Air Capture of CO(2) using Amine-Impregnated MIL-101(Cr) Enables Ambient Temperature CO(2) Recovery. *JACS Au* **2022**, *2*, 380−393.
(22) Wang, Y.; Rim, G.; Song, M.; Holmes, H. E.; Jones, C. W.; Lively, R. P. Cold Temperature Direct Air CO(2) Capture with Amine-Loaded Metal-Organic Framework Monoliths. *ACS Appl. Mater. Interfaces* **2024**, *16*, 1404.
(23) Andrade, M.; Li, S.; Varni, A. J.; Russell-Parks, G. A.; Braunecker, W. A.; Hunters-Sellars, E.; et al. Enhanced Hydrogen Bonding via Epoxide-functionalization Restricts Mobility in Poly(ethylenimine) for CO2 Capture. *Chem. Commun.* **2023**, *59*, 10737.
(24) Min, K.; Choi, W.; Kim, C.; Choi, M. Oxidation-stable amine-containing adsorbents for carbon dioxide capture. *Nat. Commun.* **2018**, *9*, 726.
(25) Park, S.; Choi, K.; Yu, H. J.; Won, Y.-J.; Kim, C.; Choi, M.; Cho, S.-H.; Lee, J.-H.; Lee, S. Y.; Lee, J. S. Thermal Stability Enhanced Tetraethylenepentamine/Silica Adsorbents for High Performance CO2 Capture. *Ind. Eng. Chem. Res.* **2018**, *57*, 4632−4639.
(26) Sakwa-Novak, M. A.; Tan, S.; Jones, C. W. Role of Additives in Composite PEI/Oxide CO(2) Adsorbents: Enhancement in the Amine Efficiency of Supported PEI by PEG in CO(2) Capture from Simulated Ambient Air. *ACS Appl. Mater. Interfaces* **2015**, *7*, 24748−24759.
(27) Elfving, J.; Bajamundi, C.; Kauppinen, J. Characterization and Performance of Direct Air Capture Sorbent. *Energy Procedia* **2017**, *114*, 6087−6101.
(28) Elfving, J.; Kauppinen, J.; Jegoroff, M.; Ruuskanen, V.; Järvinen, L.; Sainio, T. Experimental comparison of regeneration methods for CO2 concentration from air using amine-based adsorbent. *Chem. Eng. J.* **2021**, *404*, No. 126337.
(29) Ünveren, E. E.; Monkul, B. Ö.; Sarıoğlan, Ş.; Karademir, N.; Alper, E. Solid amine sorbents for CO2 capture by chemical adsorption: A review. *Petroleum* **2017**, *3*, 37−50.
(30) Marle de Jong, M. B.; Hamelinck, C. *Methanol carbon footprint and certification*; Methanol Institute: 2022.
(31) Klinthong, W.; Huang, C.-H.; Tan, C.-S. One-Pot Synthesis and Pelletizing of Polyethylenimine-Containing Mesoporous Silica Powders for CO2 Capture. *Ind. Eng. Chem. Res.* **2016**, *55*, 6481−6491.
(32) Quang, D. V.; Dindi, A.; Abu-Zahra, M. R. M. One-Step Process Using CO2 for the Preparation of Amino-Functionalized Mesoporous Silica for CO2 Capture Application. *ACS Sustainable Chem. Eng.* **2017**, *5*, 3170−3178.
(33) Rezaei, F.; Sakwa-Novak, M. A.; Bali, S.; Duncanson, D. M.; Jones, C. W. Shaping amine-based solid CO2 adsorbents: Effects of pelletization pressure on the physical and chemical properties. *Microporous Mesoporous Mater.* **2015**, *204*, 34−42.
(34) Thakkar, H.; Eastman, S.; Al-Mamoori, A.; Hajari, A.; Rownaghi, A. A.; Rezaei, F. Formulation of Aminosilica Adsorbents into 3D-Printed Monoliths and Evaluation of Their CO(2) Capture Performance. *ACS Appl. Mater. Interfaces* **2017**, *9*, 7489−7498.
(35) Ahmadian Hosseini, A.; Jahandar Lashaki, M. A comprehensive evaluation of amine-impregnated silica materials for direct air capture of carbon dioxide. *Sep. Purif. Technol.* **2023**, *325*, No. 124580.
(36) Li, C.; Wang, X.; Yang, A.; Chen, P.; Zhao, T.; Liu, F. Polyethyleneimine-Modified Amorphous Silica for the Selective Adsorption of CO(2)/N(2) at High Temperatures. *ACS Omega* **2021**, *6*, 35389−35397.
(37) Sakwa-Novak, M. A.; Yoo, C. J.; Tan, S.; Rashidi, F.; Jones, C. W. Poly(ethylenimine)-Functionalized Monolithic Alumina Honeycomb Adsorbents for CO2 Capture from Air. *ChemSusChem* **2016**, *9*, 1859−1868.
(38) *U.S. Average Humidity State Rank*, 2024, USA.com.
(39) Russell-Parks, G. A.; Leick, N.; Marple, M. A. T.; Strange, N. A.; Trewyn, B. G.; Pang, S. H.; Braunecker, W. A. Fundamental Insight into Humid CO2 Uptake in Direct Air Capture Nanocomposites Using Fluorescence and Portable NMR Relaxometry. *J. Phys. Chem. C* **2023**, *127*, 15363−15374.
(40) Sayari, A.; Belmabkhout, Y. Stabilization of amine-containing CO2 adsorbents: Dramatic effect of water vapor. *J. Am. Chem. Soc.* **2010**, *132*, 6312−6314.
(41) Wang, Y.; Hu, X.; Guo, T.; Tian, W.; Hao, J.; Guo, Q. The competitive adsorption mechanism of CO2, H2O and O2 on a solid amine adsorbent. *Chem. Eng. J.* **2021**, *416*, No. 129007.

https://doi.org/10.1021/acsomega.4c05639
ACS Omega 2024, 9, 45970−45982

(42) Cherevotan, A.; Raj, J.; Peter, S. C. An overview of porous silica immobilized amines for direct air CO2 capture. *J. Mater. Chem. A* **2021**, *9*, 27271−27303.
(43) Thakkar, H.; Eastman, S.; Al-Naddaf, Q.; Rownaghi, A. A.; Rezaei, F. 3D-Printed Metal-Organic Framework Monoliths for Gas Adsorption Processes. *ACS Appl. Mater. Interfaces* **2017**, *9*, 35908−35916.
(44) Thakkar, H.; Eastman, S.; Hajari, A.; Rownaghi, A. A.; Knox, J. C.; Rezaei, F. 3D-Printed Zeolite Monoliths for CO(2) Removal from Enclosed Environments. *ACS Appl. Mater. Interfaces* **2016**, *8*, 27753−27761.

https://doi.org/10.1021/acsomega.4c05639
ACS Omega 2024, 9, 45970−45982